Structural characterization, magnetic and Magnetocaloric Measurements on the iron pyrophosphate $KFeP_2O_7$

Assaad Elouafi[1], Sara Ezairi[2], Fatima Lmai[2], Abdeslam Tizliouine[1]

[1]*LMPGI, Université Hassan II de Casablanca, Ecole Supérieure de Technologie (ESTC), Casablanca, Morocco.*
[2]*LPMAT, Faculty of Sciences Ain Chock, Hassan II University of Casablanca, Casablanca, Morocco.*

Abstract

The structural, magnetic, and magnetocaloric characteristics of potassium diphosphate KCrP2O7 were thoroughly investigated. A solid-state reaction method has been employed to synthesize this specimen. The crystalline structure was analysed employing X-Ray Diffraction (XRD), infrared, and Raman spectroscopy at around room temperature. Detailed Rietveld refinement analysis reveals that the compound adopts a complex monoclinic structure with the space group P21/c and the lattice parameters: a = 7.357Å, b = 10.011 Å, and c = 8.202 Å. The Magnetic measurements exhibit an antiferromagnetic-paramagnetic behavior with a second order magnetic transition near the Néel temperature TN (TN = 8.5 K) for KCrP2O7. Magnetic entropy change (-ΔSM) induced by the magnetic field, was determined by employing the thermodynamic Maxwell's relation. At H=50 kOe, the ($-\Delta S_M^{Max}$) and RCP (magnetic refrigeration capacity) near T_N show a value of 4.4 J.kg-1 .K-1 and 30.06 J.kg-1, respectively for the KCrP2O7 compound.

Methods

To prepare the $KCrP_2O_7$ fine powder, the solid-state reaction method was employed. The starting reagents K_2CO_3, Cr_2O_3, and $NH_4H_2PO_4$ were correctly calculated in the desired proportion. Firstly, weighted amounts of starting materials were all mixed homogeneously in an agate mortar for 4 h and progressively pre-heated primarily from room temperature to 573 K for 8 h with intermediate regrinding to exhaust NH_3, H_2O, and CO_2. Secondly, the calcined powders were all uniaxially pressed into a cylindrical pellet (diameter ≈10 mm and thickness≈0.1mm) employing a hydraulic press and then the pellets were sintered at an optimized temperature 973 K for 12 h to acquire close packed grains and characterized by X-ray diffractometer using Siemens D5000 equipment with Cu-$K_{\alpha 1}$ radiation (λ = 1.5406 Å). The actual magnetic measurements were performed employing a superconducting quantum interference device (SQUID) sensor (MPMS-XL-7AC, Quantum Design). Zero field-cooled (ZFC) curve was obtained by applying a magnetic field of 500 Oe and varying the temperature from 2 K to 100 K. Magnetization versus of the applied magnetic field was provided at temperatures with 3 <T<30 K, with a maximum applied field up to 50 kOe. The variation in the morphology and particle size was estimated from FEI ESEM Quanta 450 FEG scanning electron microscopy.

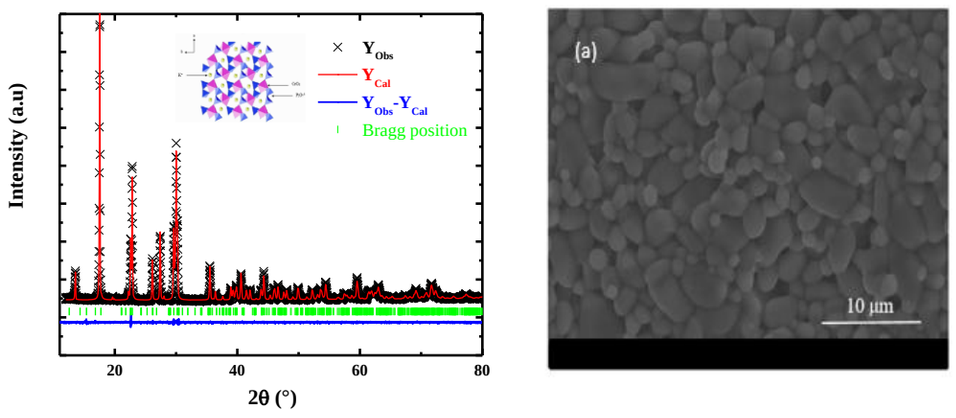

Fig. 1 : Remarked and calculated X-ray powder diffraction patterns for $KCrP_2O_7$. Reflection positions are marked for the phase. The Illustrations represent the packing of the molecules of $KCrP_2O_7$ below the c-axis (inset Fig. 1). **Fig. 2** SEM of the KCrP2O7 sample

Fig. 1 exhibits the XRPD pattern of $KCrP_2O_7$ powder. The remarked peaks actually imply a polycrystalline character of the sample with steps of 0.01° (2θ), in the 2θ range of 15-80° with a fixed-time counting of 2 seconds/step. This figure showed no detectable spurious phase in the (XRD) limit. Diffraction data were collected and analyzed by the Rietveld technique employing the Fullprof program inserted in Winplotr software. The Rietveld refinement, as marked by available data of powder XRD, is initiated with the scale and background parameters.SEM (Sscanning Electron Microscope) was also used to verify the morphology of the KCrP2O7 sample. As depicted in Fig. 2, the main morphology of this sample was the huge grain size in various shapes and the average grain size up to 1.2 µm. However, the particles remarked by SEM should have a number of polycrystalline diffracting grains. Fig. 2a depicts the chemical composition analysis results of the KCrP2O7 compound.

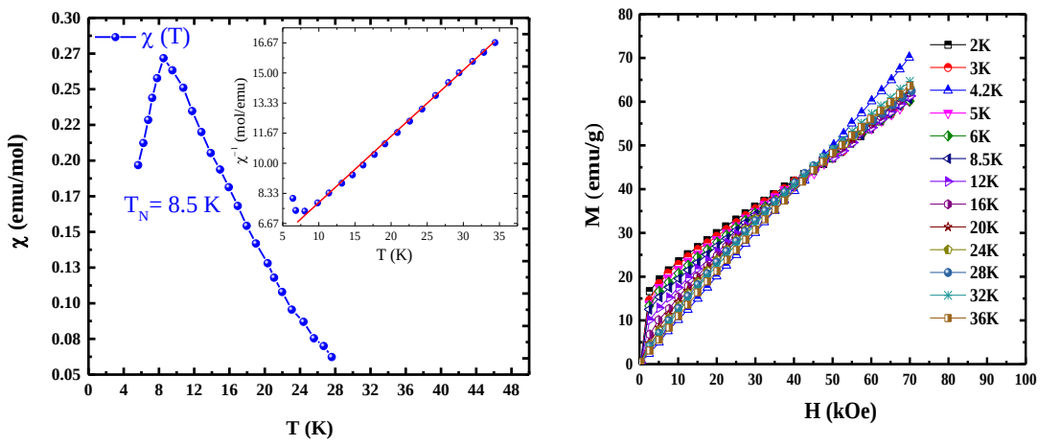

Fig. 3: Temperature change with magnetic susceptibility and the inverse magnetic susceptibility (inset Fig.3) under 50 Oe; **Fig. 4**: M(H) curves directly measured at various temperatures of KCrP2O7

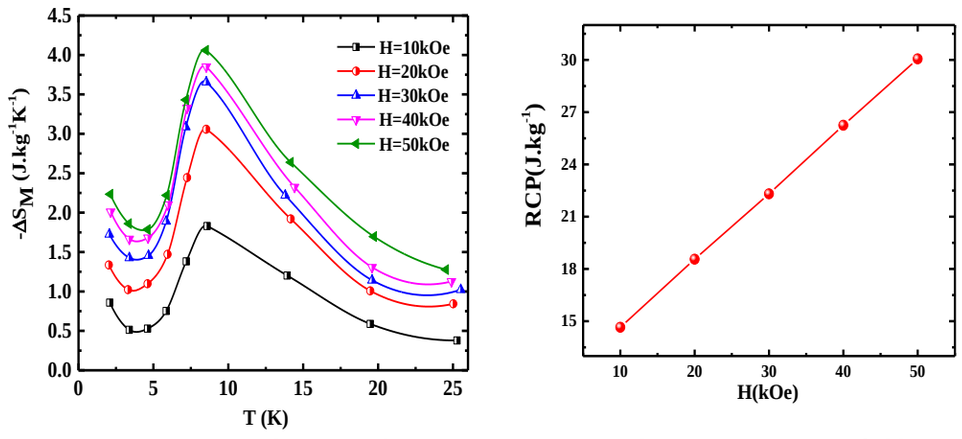

Fig. 5: Magnetic entropy changes with temperatures, measured at various magnetic field H; **Fig. 6**: Variation magnetic field with magnetic refrigeration capacity (RCP) of $KCrP_2O_7$ sample.

In Fig. 3 the change of the magnetic susceptibility χ (T) and inverse susceptibility χ^{-1}(T) versus temperature is directly measured under a magnetic field intensity of 500 Oe. As we can see, the magnetic susceptibility increases as the temperature increases at low temperatures, reaching a maximum around T_N. So, this comportment is a fairly typical signature of an antiferromagnetic (AFM) material. It is really clear from the measurements that the compound displays an antiferromagnetic-paramagnetic (AFM-PM) transition in vicinity of T_N=8.5 K [1]. Using Curie-Weiss law and in this way, we can make the line fit paramagnetic region of the χ^{-1}(T) through the following expressions [2]:

$$\chi = \frac{C}{T - \theta_p} \qquad (1)$$

Results

Where θ_p and C are the Curie-Weiss temperature and Curie constant, respectively. The values of C and θ_p are also obtained from the linear fit of the equation (1). The value of θ_p (θ_p = -36 K) is negative, underlining the appearance of an AFM interaction between Cr^{3+} ions. We have inferred the effective moment experimental μ_{eff}^{Exp} values from the Curie constant employing the following relationship represented as [3]:

$$\left(\mu_{eff}^{Exp}\right)^2 = \frac{3\,k_B}{N_A\,\mu_B^2}\,C \qquad (2)$$

Where k_B, μ_B, and N_A are the Boltzmann constant, Bohr magneton and Avogadro number, respectively. The obtained experimental value of μ_{eff}^{Exp} is 3.53 μ_B, which is close to the theoretical value of $\mu_{eff.}^{The}$ ($\mu_{eff.}^{The}$ = 3.87 μ_B).

Fig. 4, shows the isothermal magnetization curves of $KCrP_2O_7$ powder controlled at regular intervals throughout a broad range of temperatures between 2 K and 36 K. The variation progressive of M(μ_0H) reveals the variation linear in the curves, which is indicate the paramagnetic contribution above T_N. Both the hysteresis loop and isothermal magnetization curves of $KCrP_2O_7$ are suitable for magnetic refrigeration [4].

It is easy to calculate the sample's magnetocaloric effect, which is related to the magnetic properties through the magnetic entropy change ($-\Delta S_M$) by employing the thermodynamic Maxwell relation, as follows [5]:

$$\Delta S_M(T,\ \Delta H)_{\Delta H} = S_M(T, H) - S_M(T,\ 0) = \int_0^{\mu_0 H_{Max}} \left(\frac{\partial M(H, T)}{\partial T}\right)_H dH \qquad (3)$$

where $\mu_0 H_{Max}$ denotes the maximum of the external magnetic applied field.

To provide a precise measurements of magnetization at various fields and temperatures, the change in magnetic entropy that is shown in equ.(3) can be approximated by the following equation [6]:

$$\Delta S_M(T, H) = \mu_0 \sum_i \frac{M_{i+1}(T_{i+1}, H) - M_i(T_i, H)}{T_{i+1} - T_i}\,\Delta H_i \qquad (4)$$

Now, under an applied magnetic field of $\mu_0\Delta H_i$, the experimental magnetization values M_i and M_{i+1} are measured at temperatures T_i and T_{i+1}, respectively.

Fig. 5 exhibits the variation of $-\Delta S_M$ vs. T for $KCrP_2O_7$ powder obtained at selected values of ΔH (10, 20, 30, 40, and 50 kOe). The maximum values of ($-\Delta S_M$) vs. T curves were actually found to be nearby T_N. The caret-like shape ($-\Delta S_M$ vs. T) clearly shows that the magnetic phase transition approaching T_N is a 2nd order (SOMT). One really can remark that the maximum peak value of ($-\Delta S_M$) rises from 1.83 to 4.07 $J.kg^{-1}.K^{-1}$ with increasing ΔH from 1 to 50 kOe, respectively. On the other hand, the increase above 25 K is probably due to the second phase transition, which was not apparent when the structure of $KCrP_2O_7$ analysed by X-Ray Powder Diffraction. The rise in ($-\Delta S_M^{Max}$) versus $\mu_0\Delta H$ can really be understood by considering the rise of magnetization near the AFM-PM transition in $KCrP_2O_7$

The magnetic refrigeration capacity (RCP) is a critical metric for an essential feature of the MCE; it is connected with the application of magnetic refrigerators. To evaluate RCP, we also used the following formula [7]:

$$RCP = -\Delta S_M^{Max}(T, H_{Max}) \times \delta T^{FWHM} \qquad (5)$$

With ($-\Delta S_M^{Max}$) denotes the maximum of the magnetic entropy change and δT^{FWHM} denotes the full width at half the maximum of the peak. One can see that the values of the RCP rise from 14.65 to 30.06 $J.kg^{-1}$ with increasing $\mu_0\Delta H$ from 1 to 50 kOe, respectively(Fig.6)

Conclusion

In this scientific research, we tried to analyze the structural, magnetic, and magnetocaloric properties of potassium diphosphate $KCrP_2O_7$ powder. The XRPD technique was confirmed a monoclinic structure with the space group P21/c and the lattice parameters: a = 7.350Å, b = 9.9691 Å, and c = 8.1832 Å.. Magnetic measurements exhibit an antiferromagnetic-paramagnetic comportment with a second order transition near the Néel temperature (T_N = 8.5 K) for $KCrP_2O_7$. Furthermore, as the magnetic field increases, the ($-\Delta S_M^{Max}$) and RCP increase. For a magnetic field of 50 kOe, and in the vicinity of the Neel temperature, the values of ($-\Delta S_M^{Max}$) and RCP are 4.4 $J.kg^{-1}.K^{-1}$ and 30.06 $J.kg^{-1}$, respectively.

Reference

1. Rajivgandhi R, Chelvane JA, Nigam AK, Malik SK, Nirmala R. Preservation of large low temperature magnetocaloric effect in metamagnetic intermetallic compounds RCu2 (R = Gd, Tb, Dy, Ho and Er) upon rapid solidification. J Alloys Compd [Internet]. 2020;815:152659. Available from: https://www.sciencedirect.com/science/article/pii/S0925838819339052

2. El Ouahbi S, Yamkane Z, Derkaoui S, Lassri H. Magnetic Properties and the Critical Exponents in Terms of the Magnetocaloric Effect of Amorphous Fe40Ni38Mo4B18 Alloy. J Supercond Nov Magn [Internet]. 2021;34:1253–7. Available from: https://doi.org/10.1007/s10948-021-05832-y

3. Zaidi MA, Dhahri J, Zeydi I, Alharbi T, Belmabrouk H. Large magnetocaloric effect and critical behavior in La0.7Ba0.2Ca0.1Mn1-: XAlxO3. RSC Adv. 2017;7:43590–9.

4. Ettayfi A, Moubah R, Boutahar A, Hlil EK, Lassri H. Structural, Magnetic, Magnetocaloric, and Critical Exponent Properties of La0.67Sr0.33MnO3 Powders Synthesized by Solid-State Reaction. J Supercond Nov Magn [Internet]. 2016;29:133–8. Available from: https://doi.org/10.1007/s10948-015-3212-5

5. Dhahri I, Ellouze M, Mnasri T, Hlil EK, Jotania RB. Structural, magnetic, magnetocaloric and critical exponents of oxide manganite La0.7Sr0.3Mn0.95Fe0.05O3. J Mater Sci Mater Electron [Internet]. 2020;31:12493–501. Available from: https://doi.org/10.1007/s10854-020-03797-7

6. Elouafi A, Moubah R, Derkaoui S, Tizliouine A, Cherkaoui R, Shi S, et al. Finite size effects on the magnetocaloric properties around blocking temperature in γ-Fe2O3 nanoparticles. Phys A Stat Mech its Appl [Internet]. 2019;523:260–7. Available from: https://www.sciencedirect.com/science/article/pii/S037843711930192X

7. ZAIDI, M. A., DHAHRI, J., ZEYDI, I. et al. Large magnetocaloric effect and critical behavior in La 0.7 Ba 0.2 Ca 0.1 Mn 1− x Al x O 3. RSC Adv. 2017;7:43590–9.